International Journal of Advanced Engineering and Management Research

Vol. 7, No. 02; 2022

ISSN: 2456-3676

Finite Element Modelling of Rotors, Without Considering the Shear Effects

Tieba Ouattara[1], Moussa Magara Traoré[2], Chaka Berthé[3]

[1, 2, 3] Ecole Normale d'Enseignement Technique et Professionnel (ENETP), Campus Universitaire de Kabala, Bâtiment N0 4, Bamako, Mali

doi: 10.51505/IJAEMR.2022.7216 URL: http://dx.doi.org/10.51505/IJAEMR.2022.7216

Abstract

The proposed rotor model is based on the finite elements of a Timoshenko beam, whose support is rigid and fixed. It takes into account the geometric asymmetry of the discs and/or the shaft, while neglecting the shear effect.

The equations of motion obtained include time-varying parametric terms that can lead to lateral dynamic instability. The influence of the combined rotational and translational movements of the support is analyzed by the Campbell diagram and the rotor stability map. Critical speeds according to modes have been identified.

Keywords: Asymmetrical rotor, Parametric excitation, finite elements, Critical speeds.

Introduction:

The shaft of a rotor with properties of inertia and mass distributed along its length can be considered as a continuous elastic body, especially for high speeds. However, the vibration problems linked to the main elements such as the shafts and the rotors are phenomena which are still of concern despite the progress made in the design. These problems are due, for example, to the inevitable defects in machining and assembly that cause various types of vibrations in this mechanical system which limit the performance of the machines by affecting their functionality and their profitability and endangering the safety of operation.

For this, various types of vibrations appear in this mechanical system, limit its performance and endanger the safety of operation. The dynamic analysis of continuous bodies in rotation is therefore essential. An understanding of the vibratory behavior and sufficient knowledge of the dynamics of the rotors are therefore essential to ensure the proper functioning of the mechanism.

In this context, the literature includes many books studying a large number of phenomena related to the dynamics of rigid/flexible and symmetrical/asymmetrical rotor systems mounted on linear/nonlinear elastic bearings in the case of a fixed support [5], [4], [2,3], [7], [1]. In this situation, the first concern is to predict the critical rotation speeds of Resonance and after modify the design to change them to avoid them.

The setting in equation is carried out by the Lagrangian; it is first necessary to write the kinetic and deformation energies of the components of the rotor; whose calculation requires some assumptions and simplifications detailed [4], [6] and [7].

These equations thus include numerous non-linearities. For the dynamic study of rotors. The hypothesis of small displacements is classically put forward, it is assumed that the speed of

Vol. 7, No. 02; 2022

ISSN: 2456-3676

rotation varies where it is an unknown function of time. The essential studies of the dynamics of the rotors concerning the plot of the Campbell diagram which represents the evolution of the natural frequencies according to the speed of rotation and the calculation of the responses to unbalance during the passage of the critical speed [6], [7], [8] and [9].
To carry out these studies, we now have many modeling tools, among them the finite element method detailed [6], [7], [8], [9], [10],[11] and [12] which takes into consideration the particularities presented by the dynamics of the rotors compared to the dynamics of the fixed structures.

Material and results:
The finite element method, as a numerical method, is known among the most important and effective methods for modeling and solving complex problems in engineering sciences, and in particular in rotor dynamics. Today it is one of the most widely used tools in numerical simulation of the behavior of structures under complex mechanical, thermal or coupled loads. Rotors are no exception to this application.

In this study we will see the modeling of the rotors by this numerical method. After having discretized the rotors in finite elements while neglecting the effects of shearing, then the equations of motion of the rotor are developed using this method, by explaining the elementary matrices of the various elements of the rotor (shaft, disc, spindle and unbalance).

- **Global equation of motion:**

After having determined the elementary matrices of the various components of the rotor, the assembly step is necessary in order to obtain the global matrices of the differential equation of motion. The differential equations of motion of a rotor are given in matrix form by:

$$[M_g]\ddot{\delta} + [C_g]\dot{\delta} + [K_g]\delta = \{F_{paliers}\} + \{F\} \quad (1)$$

$[M_g]$: Global mass matrix

$[C_g]$: Global damping matrix

$[K_g]$: Global stiffness matrix

$\{F_{paliers}\}$: Bearing force vector

$$\{F_{paliers}\} = \begin{Bmatrix} F_{kax} \\ F_{kaz} \end{Bmatrix}_i + \begin{Bmatrix} F_{cax} \\ F_{caz} \end{Bmatrix}_i \quad i = 1,2,\dots,n \text{ (n bearings)} \quad (2)$$

$\{F\}$: Excitation forces vector

Vol. 7, No. 02; 2022

ISSN: 2456-3676

– **Expanded form of the equation with variable speed$\dot{\varphi}$:**

$$[M_g]\ddot{\delta} + ([C_p] + \dot{\varphi}[G_g])\dot{\delta} + ([K_p] + [K_a] + \ddot{\varphi}[K_d])\delta = F_b \quad (3)$$

with:

$$[C_g] = [C_p] + \dot{\varphi}[G_g] \; ; [K_g] = [K_p] + [K_a] + \ddot{\varphi}[K_d]$$

where:

$[M_g]$: global mass matrix which includes the elementary mass matrixes of the disc Md and of the shaft$M_a = M_i^a + M_s^a$.

$[G_g]$global gyroscopic matrix including the elementary gyroscopic matrices of the disk $C_d$and the shaftC_a.

$[K_a]$: stiffness matrix of the shaft.

$[C_p]$et$[K_p]$: damping and stiffness matrices of the bearings.

$[K_d]$: disc stiffness matrix

F_b : unbalance forces vector.

$\dot{\varphi}$: rotation speed rd/s.

○ **Global matrices (application to a brushless motor):**

Consider the studied rotor model which is schematized in Figure1 having four nodes and five elements: a disc element, two bearing elements and three shaft elements of the same length: $l = l_1 = l_2 = l_3 = L/3$

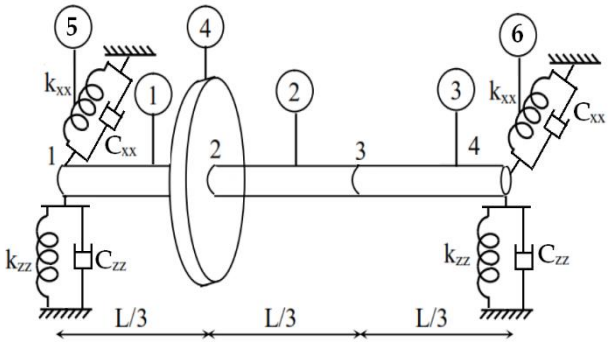

Vol. 7, No. 02; 2022

ISSN: 2456-3676

Figure1: Rotor model with elements and nodes.

In the model shown above, the nodes of each element of the shaft, bearing or disc are related to the nodes of the rotor according to the following table1 below:

Table1:

Element number	Element Type	Rotor nodes	Displacement vectors δ
1	shaft	1-2	$u_1, w_1, \theta_1, \psi_1, u_2, w_2, \theta_2, \psi_2$
2	shaft	2-3	$u_2, w_2, \theta_2, \psi_2, u_3, w_3, \theta_3, \psi_3$
3	shaft	3-4	$u_3, w_3, \theta_3, \psi_3, u_4, w_4, \theta_4, \psi_4$
4	disc	2	$u_2, w_2, \theta_2, \psi_2$
5	bearing	1	u_1, w_1
6	bearing	4	u_4, w_4

- **Shaft matrices**

The use of Lagrange's method gives:

$$\frac{d}{dt}\left(\frac{\partial T_a}{\partial \dot{\delta}}\right) - \frac{\partial T_a}{\partial \delta} = [M_i^a + M_S^a]\ddot{\delta} + \dot{\varphi} C_a \dot{\delta} + \ddot{\varphi} K_s^a \delta \quad (4)$$

The total matrices of mass, rigidity and Coriolis are obtained by superimposing the elementary matrices according to the table. Each type of global matrix is obtained by summing the three matrices of the three elements.

- **Classic global matrix of mass (M_i^a)**

The matrix with terms is given by:

$$M_i^a \delta = \frac{\rho_a s l}{420} \begin{bmatrix} 156 & 0 & 0 & -22l & 54 & 0 & 0 & 13l & 0 & 0 & 0 & 0 & 0 & 0 & 0 & 0 \\ 0 & 156 & 22l & 0 & 0 & 54 & -13l & 0 & 0 & 0 & 0 & 0 & 0 & 0 & 0 & 0 \\ 0 & 22l & 4l^2 & 0 & 0 & 13l & -3l^2 & 0 & 0 & 0 & 0 & 0 & 0 & 0 & 0 & 0 \\ -22l & 0 & 0 & 4l^2 & -13l & 0 & 0 & -3l^2 & 0 & 0 & 0 & 0 & 0 & 0 & 0 & 0 \\ 54 & 0 & 0 & -13l & 312 & 0 & 0 & 0 & 54 & 0 & 0 & 13l & 0 & 0 & 0 & 0 \\ 0 & 54 & 13l & 0 & 0 & 312 & 0 & 0 & 0 & 54 & -13l & 0 & 0 & 0 & 0 & 0 \\ 0 & -13l & -3l^2 & 0 & 0 & 0 & 8l^2 & 0 & 0 & 13l & -3l^2 & 0 & 0 & 0 & 0 & 0 \\ 13l & 0 & 0 & -3l^2 & 0 & 0 & 0 & 8l^2 & -13l & 0 & 0 & -3l^2 & 0 & 0 & 0 & 0 \\ 0 & 0 & 0 & 0 & 54 & 0 & 0 & -13l & 312 & 0 & 0 & 0 & 54 & 0 & 0 & 13l \\ 0 & 0 & 0 & 0 & 0 & 54 & 13l & 0 & 0 & 312 & 0 & 0 & 0 & 54 & -13l & 0 \\ 0 & 0 & 0 & 0 & 0 & -13l & -3l^2 & 0 & 0 & 0 & 8l^2 & 0 & 0 & 13l & -3l^2 & 0 \\ 0 & 0 & 0 & 0 & 13l & 0 & 0 & -3l^2 & 0 & 0 & 0 & 8l^2 & -13l & 0 & 0 & -3l^2 \\ 0 & 0 & 0 & 0 & 0 & 0 & 0 & 0 & 54 & 0 & 0 & -13l & 156 & 0 & 0 & 22l \\ 0 & 0 & 0 & 0 & 0 & 0 & 0 & 0 & 0 & 54 & 13l & 0 & 0 & 156 & -22l & 0 \\ 0 & 0 & 0 & 0 & 0 & 0 & 0 & 0 & 0 & -13l & -3l^2 & 0 & 0 & -22l & 4l^2 & 0 \\ 0 & 0 & 0 & 0 & 0 & 0 & 0 & 0 & 13l & 0 & 0 & -3l^2 & 22l & 0 & 0 & 4l^2 \end{bmatrix} \begin{bmatrix} \ddot{u}_1 \\ \ddot{w}_1 \\ \ddot{\theta}_1 \\ \ddot{\psi}_1 \\ \ddot{u}_2 \\ \ddot{w}_2 \\ \ddot{\theta}_2 \\ \ddot{\psi}_2 \\ \ddot{u}_3 \\ \ddot{w}_3 \\ \ddot{\theta}_3 \\ \ddot{\psi}_3 \\ \ddot{u}_4 \\ \ddot{w}_4 \\ \ddot{\theta}_4 \\ \ddot{\psi}_4 \end{bmatrix}$$

Where $\rho_a = 7800\ kg/m^3$,$s = 3{,}142.10^{-6}\mathrm{m}^2$ et l=L/3=0,0167 m^2

- **Global matrix representing the rotational inertia side effect** (M_s^a)

$$M_s^a\ddot{\delta} = \frac{\rho_a I_s}{30l}\begin{bmatrix}
36 & 0 & 0 & -3l & -36 & 0 & 0 & -3l & 0 & 0 & 0 & 0 & 0 & 0 & 0 & 0 \\
0 & 36 & 3l & 0 & 0 & -36 & 3l & 0 & 0 & 0 & 0 & 0 & 0 & 0 & 0 & 0 \\
0 & 3l & 4l^2 & 0 & 0 & -3l & -l^2 & 0 & 0 & 0 & 0 & 0 & 0 & 0 & 0 & 0 \\
-3l & 0 & 0 & 4l^2 & 36l & 0 & 0 & -l^2 & 0 & 0 & 0 & 0 & 0 & 0 & 0 & 0 \\
-36 & 0 & 0 & 3l & 72 & 0 & 0 & 0 & -36 & 0 & 0 & -3l & 0 & 0 & 0 & 0 \\
0 & -36 & -3l & 0 & 0 & 72 & 0 & 0 & 0 & -36 & 3l & 0 & 0 & 0 & 0 & 0 \\
0 & 3l & -l^2 & 0 & 0 & 0 & 8l^2 & 0 & 0 & -3l & -l^2 & 0 & 0 & 0 & 0 & 0 \\
-3l & 0 & 0 & -l^2 & 0 & 0 & 0 & 8l^2 & 3l & 0 & 0 & -l^2 & 0 & 0 & 0 & 0 \\
0 & 0 & 0 & 0 & -36 & 0 & 0 & 3l & 72 & 0 & 0 & 0 & -36 & 0 & 0 & -3l \\
0 & 0 & 0 & 0 & 0 & -36 & -3l & 0 & 0 & 72 & 0 & 0 & 0 & -36 & 3l & 0 \\
0 & 0 & 0 & 0 & 0 & 3l & -l^2 & 0 & 0 & 0 & 8l^2 & 0 & 0 & -3l & -l^2 & 0 \\
0 & 0 & 0 & 0 & -3l & 0 & 0 & -l^2 & 0 & 0 & 0 & 8l^2 & 3l & 0 & 0 & -l^2 \\
0 & 0 & 0 & 0 & 0 & 0 & 0 & 0 & -36 & 0 & 0 & 3l & 36 & 0 & 0 & 3l \\
0 & 0 & 0 & 0 & 0 & 0 & 0 & 0 & 0 & -36 & -3l & 0 & 0 & 36 & -3l & 0 \\
0 & 0 & 0 & 0 & 0 & 0 & 0 & 0 & 0 & 3l & -l^2 & 0 & 0 & -3l & 4l^2 & 0 \\
0 & 0 & 0 & 0 & 0 & 0 & 0 & 0 & -3l & 0 & 0 & -l^2 & 3l & 0 & 0 & 4l^2
\end{bmatrix}\begin{bmatrix}\ddot{u}_1\\ \ddot{w}_1\\ \ddot{\theta}_1\\ \ddot{\psi}_1\\ \ddot{u}_2\\ \ddot{w}_2\\ \ddot{\theta}_2\\ \ddot{\psi}_2\\ \ddot{u}_3\\ \ddot{w}_3\\ \ddot{\theta}_3\\ \ddot{\psi}_3\\ \ddot{u}_4\\ \ddot{w}_4\\ \ddot{\theta}_4\\ \ddot{\psi}_4\end{bmatrix}$$

$l_1= l_2=l_3=L/3=0,\ 0167\ m^2$

- **Global matrix representing the gyroscopic effect** (C_a)

$$\dot{\varphi}C_a\delta = \frac{\rho_a I_s\dot{\varphi}}{15l}\begin{bmatrix}
0 & -36 & -3l & 0 & 0 & 36 & -3l & 0 & 0 & 0 & 0 & 0 & 0 & 0 & 0 & 0 \\
36 & 0 & 0 & -3l & -36 & 0 & 0 & -3l & 0 & 0 & 0 & 0 & 0 & 0 & 0 & 0 \\
3l & 0 & 0 & -4l^2 & -3l & 0 & 0 & l^2 & 0 & 0 & 0 & 0 & 0 & 0 & 0 & 0 \\
0 & 3l & 4l^2 & 0 & 0 & -3l & -l^2 & 0 & 0 & 0 & 0 & 0 & 0 & 0 & 0 & 0 \\
0 & 36 & 3l & 0 & 0 & -72 & 0 & 0 & 0 & 36 & -3l & 0 & 0 & 0 & 0 & 0 \\
-36 & 0 & 0 & 3l & 72 & 0 & 0 & 0 & -36 & 0 & 0 & -3l & 0 & 0 & 0 & 0 \\
3l & 0 & 0 & l^2 & 0 & 0 & 0 & -8l^2 & -3l & 0 & 0 & -4l^2 & 0 & 0 & 0 & 0 \\
0 & 3l & -l^2 & 0 & 0 & 0 & 8l^2 & 0 & 0 & -3l & -l^2 & 0 & 0 & 0 & 0 & 0 \\
0 & 0 & 0 & 0 & 0 & 36 & 3l & 0 & 0 & -72 & 0 & 0 & 0 & 36 & -3l & 0 \\
0 & 0 & 0 & 0 & -36 & 0 & 0 & 3l & 72 & 0 & 0 & 0 & -36 & 0 & 0 & -3l \\
0 & 0 & 0 & 0 & 3l & 0 & 0 & l^2 & 0 & 0 & 0 & -8l^2 & -3l & 0 & 0 & l^2 \\
0 & 0 & 0 & 0 & 0 & 3l & -l^2 & 0 & 0 & 0 & 8l^2 & 0 & 0 & -3l & -l^2 & 0 \\
0 & 0 & 0 & 0 & 0 & 0 & 0 & 0 & 0 & 36 & 3l^2 & 0 & 0 & -36 & 3l & 0 \\
0 & 0 & 0 & 0 & 0 & 0 & 0 & 0 & -36 & 0 & 0 & 3l & 36 & 0 & 0 & 3l \\
0 & 0 & 0 & 0 & 0 & 0 & 0 & 0 & 3l & 0 & 0 & l^2 & -3l & 0 & 0 & -4l^2 \\
0 & 0 & 0 & 0 & 0 & 0 & 0 & 0 & 0 & 3l & -l^2 & 0 & 0 & -3l & 4l^2 & 0
\end{bmatrix}\begin{bmatrix}\dot{u}_1\\ \dot{w}_1\\ \dot{\theta}_1\\ \dot{\psi}_1\\ \dot{u}_2\\ \dot{w}_2\\ \dot{\theta}_2\\ \dot{\psi}_2\\ \dot{u}_3\\ \dot{w}_3\\ \dot{\theta}_3\\ \dot{\psi}_3\\ \dot{u}_4\\ \dot{w}_4\\ \dot{\theta}_4\\ \dot{\psi}_4\end{bmatrix}$$

- **Stiffness matrix due to the gyroscopic effect (K_s^a)**

$$\varphi K_s^a \delta = \frac{\rho_a I_s \varphi}{15l(1+\zeta)^2}$$

$$\begin{bmatrix}
0 & -36 & -3l & 0 & 0 & 36 & -3l & 0 & 0 & 0 & 0 & 0 & 0 & 0 & 0 & 0 \\
0 & 0 & 0 & 0 & 0 & 0 & 0 & 0 & 0 & 0 & 0 & 0 & 0 & 0 & 0 & 0 \\
0 & 0 & 0 & 0 & 0 & 0 & 0 & 0 & 0 & 0 & 0 & 0 & 0 & 0 & 0 & 0 \\
0 & 3l & 4l^2 & 0 & 0 & -3l & -l^2 & 0 & 0 & 0 & 0 & 0 & 0 & 0 & 0 & 0 \\
0 & 36 & 3l & 0 & 0 & -72 & 0 & 0 & 0 & 36 & -3l & 0 & 0 & 0 & 0 & 0 \\
0 & 0 & 0 & 0 & 0 & 0 & 0 & 0 & 0 & 0 & 0 & 0 & 0 & 0 & 0 & 0 \\
0 & 0 & 0 & 0 & 0 & 0 & 0 & 0 & 0 & 0 & 0 & 0 & 0 & 0 & 0 & 0 \\
0 & 3l & -l^2 & 0 & 0 & 0 & 8l^2 & 0 & 0 & -3l & -l^2 & 0 & 0 & 0 & 0 & 0 \\
0 & 0 & 0 & 0 & 0 & 36 & 3l & 0 & 0 & -72 & 0 & 0 & 0 & 36 & -3l & 0 \\
0 & 0 & 0 & 0 & 0 & 0 & 0 & 0 & 0 & 0 & 0 & 0 & 0 & 0 & 0 & 0 \\
0 & 0 & 0 & 0 & 0 & 0 & 0 & 0 & 0 & 0 & 0 & 0 & 0 & 0 & 0 & 0 \\
0 & 0 & 0 & 0 & 0 & 3l & -l^2 & 0 & 0 & 0 & 8l^2 & 0 & 0 & -3l & -l^2 & 0 \\
0 & 0 & 0 & 0 & 0 & 0 & 0 & 0 & 0 & 36 & 3l & 0 & 0 & -36 & 3l & 0 \\
0 & 0 & 0 & 0 & 0 & 0 & 0 & 0 & 0 & 0 & 0 & 0 & 0 & 0 & 0 & 0 \\
0 & 0 & 0 & 0 & 0 & 0 & 0 & 0 & 0 & 0 & 0 & 0 & 0 & 0 & 0 & 0 \\
0 & 0 & 0 & 0 & 0 & 0 & 0 & 0 & 0 & 3l & -l^2 & 0 & 0 & -3l & 4l^2 & 0
\end{bmatrix}
\begin{bmatrix} u_1 \\ w_1 \\ \theta_1 \\ \psi_1 \\ u_2 \\ w_2 \\ \theta_2 \\ \psi_2 \\ u_3 \\ w_3 \\ \theta_3 \\ \psi_3 \\ u_4 \\ w_4 \\ \theta_4 \\ \psi_4 \end{bmatrix}$$

- **Strain Energy Total Stiffness Matrix**

$$k_a = \frac{E_a I_s}{l^3}$$

$$\begin{bmatrix}
12 & 0 & 0 & -6l & -12 & 0 & 0 & -6l & 0 & 0 & 0 & 0 & 0 & 0 & 0 & 0 \\
0 & 12 & 6l & 0 & 0 & -12 & 6l & 0 & 0 & 0 & 0 & 0 & 0 & 0 & 0 & 0 \\
0 & 6l & 4l^2 & 0 & 0 & -6l & 2l^2 & 0 & 0 & 0 & 0 & 0 & 0 & 0 & 0 & 0 \\
-6l & 0 & 0 & 4l^2 & 6l & 0 & 0 & 2l^2 & 0 & 0 & 0 & 0 & 0 & 0 & 0 & 0 \\
-12 & 0 & 0 & 6l & 24 & 0 & 0 & 0 & -12 & 0 & 0 & -6l & 0 & 0 & 0 & 0 \\
0 & -12 & -6l & 0 & 0 & 24 & 0 & 0 & 0 & -12 & 6l & 0 & 0 & 0 & 0 & 0 \\
0 & 6l & 2l^2 & 0 & 0 & 0 & 8l^2 & 0 & 0 & -6l & 2l^2 & 0 & 0 & 0 & 0 & 0 \\
-6l & 0 & 0 & 2l^2 & 0 & 0 & 0 & 8l^2 & 6l & 0 & 0 & 2l^2 & 0 & 0 & 0 & 0 \\
0 & 0 & 0 & 0 & -12 & 0 & 0 & 6l & 24 & 0 & 0 & 0 & -12 & 0 & 0 & -6l \\
0 & 0 & 0 & 0 & 0 & -12 & -6l & 0 & 0 & 24 & 0 & 0 & 0 & -12 & 6l & 0 \\
0 & 0 & 0 & 0 & 0 & 6l & 2l^2 & 0 & 0 & 0 & 8l^2 & 0 & 0 & -6l & 2l^2 & 0 \\
0 & 0 & 0 & 0 & -6l & 0 & 0 & 2l^2 & 0 & 0 & 0 & 8l^2 & 6l & 0 & 0 & 2l^2 \\
0 & 0 & 0 & 0 & 0 & 0 & 0 & 0 & -12 & 0 & 0 & 6l & 12 & 0 & 0 & 6l \\
0 & 0 & 0 & 0 & 0 & 0 & 0 & 0 & 0 & -12 & 6l & 0 & 0 & 12 & -6l & 0 \\
0 & 0 & 0 & 0 & 0 & 0 & 0 & 0 & 0 & 6l & 2l^2 & 0 & 0 & -6l & 4l^2 & 0 \\
0 & 0 & 0 & 0 & 0 & 0 & 0 & 0 & -6l & 0 & 0 & 2l^2 & 6l & 0 & 0 & 4l^2
\end{bmatrix}
\begin{bmatrix} u_1 \\ w_1 \\ \theta_1 \\ \psi_1 \\ u_2 \\ w_2 \\ \theta_2 \\ \psi_2 \\ u_3 \\ w_3 \\ \theta_3 \\ \psi_3 \\ u_4 \\ w_4 \\ \theta_4 \\ \psi_4 \end{bmatrix}$$

With $I_s=1,57.10^{-12}$ m^4,et $E=2.10^{11}$Pa

Vol. 7, No. 02; 2022

ISSN: 2456-3676

- **Bearing matrix**

• at node 1:at node 4:

$$\{F_{palier(5)}\} = \begin{bmatrix} F_{u_{51}} \\ F_{w_{51}} \\ F_{\theta_{51}} \\ F_{\psi_{51}} \\ F_{u_{52}} \\ F_{w_{52}} \\ F_{\theta_{52}} \\ F_{\psi_{52}} \\ F_{u_{53}} \\ F_{w_{53}} \\ F_{\theta_{53}} \\ F_{\psi_{53}} \\ F_{u_{54}} \\ F_{w_{54}} \\ F_{\theta_{54}} \\ F_{\psi_{54}} \end{bmatrix} = \begin{bmatrix} -10^6.u \\ -10^6.w \\ 0 \\ 0 \\ 0 \\ 0 \\ 0 \\ 0 \\ 0 \\ 0 \\ 0 \\ 0 \\ 0 \\ 0 \\ 0 \\ 0 \end{bmatrix} \quad \{F_{palier(6)}\} = \begin{bmatrix} F_{u_{61}} \\ F_{w_{61}} \\ F_{\theta_{61}} \\ F_{\psi_{61}} \\ F_{u_{62}} \\ F_{w_{62}} \\ F_{\theta_{62}} \\ F_{\psi_{62}} \\ F_{u_{63}} \\ F_{w_{63}} \\ F_{\theta_{63}} \\ F_{\psi_{63}} \\ F_{u_{64}} \\ F_{w_{64}} \\ F_{\theta_{64}} \\ F_{\psi_{64}} \end{bmatrix} = \begin{bmatrix} 0 \\ 0 \\ 0 \\ 0 \\ 0 \\ 0 \\ 0 \\ 0 \\ 0 \\ 0 \\ 0 \\ 0 \\ -10^6.u \\ -10^6.w \\ 0 \\ 0 \end{bmatrix}$$

Where $F_{u_{xy}} = \{forceFindirectionuappliedtoelementxatnodey\}$

- **Unbalance matrix**

$$\{F_{balourd}\} = \begin{bmatrix} F_{u_{41}} \\ F_{w_{41}} \\ F_{\theta_{41}} \\ F_{\psi_{41}} \\ F_{u_{42}} \\ F_{w_{42}} \\ F_{\theta_{42}} \\ F_{\psi_{42}} \\ F_{u_{43}} \\ F_{w_{43}} \\ F_{\theta_{43}} \\ F_{\psi_{43}} \\ F_{u_{44}} \\ F_{w_{44}} \\ F_{\theta_{44}} \\ F_{\psi_{44}} \end{bmatrix} = \begin{bmatrix} 0 \\ 0 \\ 0 \\ 0 \\ 2.10^{-6}\ddot{\varphi}\cos\varphi - 2.10^{-6}\dot{\varphi}^2\sin\varphi \\ 2.10^{-6}\ddot{\varphi}\sin\varphi - 2.10^{-6}\dot{\varphi}^2\cos\varphi \\ 0 \\ 0 \\ 0 \\ 0 \\ 0 \\ 0 \\ 0 \\ 0 \\ 0 \\ 0 \end{bmatrix}$$

$$\{F_{balourd}\} = \begin{Bmatrix} F_u \\ F_w \\ F_\theta \\ F_\psi \end{Bmatrix} = \begin{Bmatrix} m_b d\ddot{\varphi}\cos\varphi - m_b d\dot{\varphi}^2\sin\varphi \\ m_b d\ddot{\varphi}\sin\varphi - m_b d\dot{\varphi}^2\cos\varphi \\ 0 \\ 0 \end{Bmatrix}$$

$$m_b d = 2.10^{-6} kg.\mathrm{m}$$

Where $F_{u_{xy}} = \{forceFindirectionuappliedtoelementxatnodey\}$

Vol. 7, No. 02; 2022

ISSN: 2456-3676

- **Global disc matrix (mass and gyroscopic)**

$$\frac{d}{dt}\left(\frac{\partial T_d}{\partial \dot{\delta}_i}\right)-\frac{\partial T_d}{\partial \delta_i}=\mathbf{M_d}\ddot{\delta}+\dot{\varphi}\mathbf{C_d}\dot{\delta}+\ddot{\varphi}\mathbf{K_d}\delta$$

$$\frac{d}{dt}\left(\frac{\partial T_d}{\partial \dot{\delta}}\right)-\frac{\partial T_d}{\partial \delta}=\begin{bmatrix} m_d & 0 & 0 & 0\\ 0 & m_d & 0 & 0\\ 0 & 0 & I_{dx} & 0\\ 0 & 0 & 0 & I_{dx}\end{bmatrix}\begin{bmatrix}\ddot{u}_2\\ \ddot{w}_2\\ \ddot{\theta}_2\\ \ddot{\psi}_2\end{bmatrix}+\dot{\varphi}\begin{bmatrix}0 & 0 & 0 & 0\\ 0 & 0 & 0 & 0\\ 0 & 0 & 0 & -I_{dy}\\ 0 & 0 & I_{dy} & 0\end{bmatrix}\begin{bmatrix}\dot{u}_2\\ \dot{w}_2\\ \dot{\theta}_2\\ \dot{\psi}_2\end{bmatrix}+\ddot{\varphi}\begin{bmatrix}0 & 0 & 0 & 0\\ 0 & 0 & 0 & 0\\ 0 & 0 & 0 & 0\\ 0 & 0 & I_{dy} & 0\end{bmatrix}\begin{bmatrix}u_2\\ w_2\\ \theta_2\\ \psi_2\end{bmatrix}$$

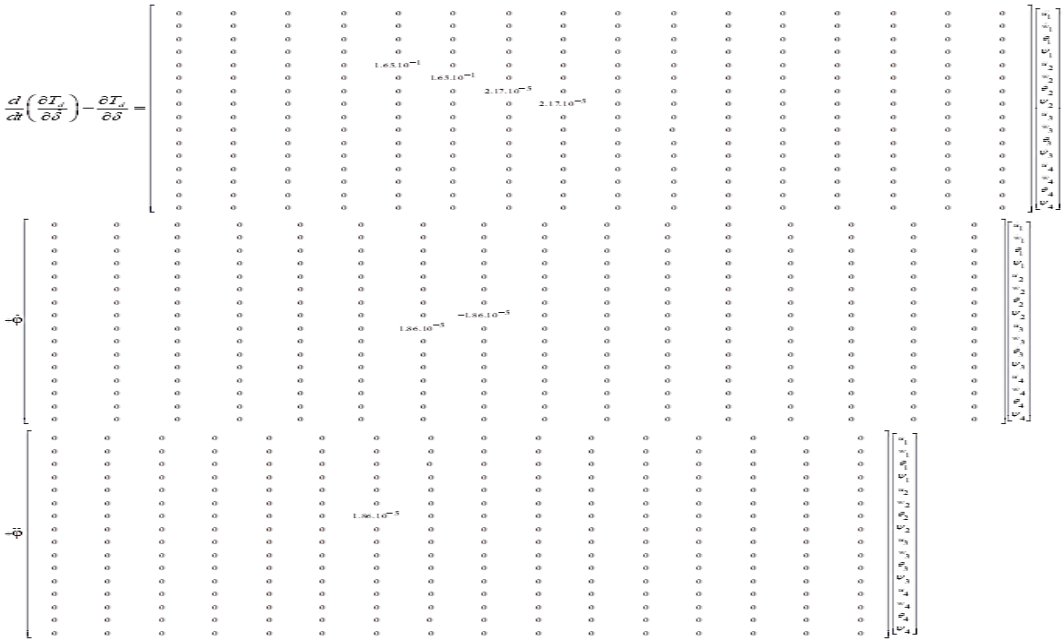

- **Simulation of the dynamic behavior of the brushless motor rotor**

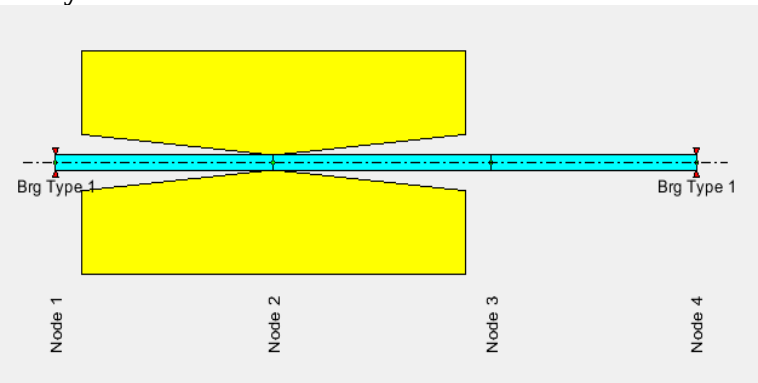

Figure1: brushless motor rotor system

This model is simulated by software which is a set of scripts written in MATLAB to accompany the book (Dynamics of Rotating Machines) [13]. Its main purpose is to illustrate the

Vol. 7, No. 02; 2022

ISSN: 2456-3676

characteristics of the rotating machines described in the book, in particular the lateral movement based on in-line shaft models. It can be used to scan other machines and for research purposes. Once the dynamic model has been developed for the brushless motor, we start by identifying the critical frequencies of the rotor through the Campbell Diagram Figure 2. The flexible rotor has two critical speeds in the range of speeds studied, these speeds are given by: cr1 =3210 rpm and cr2 = 10297rpm.

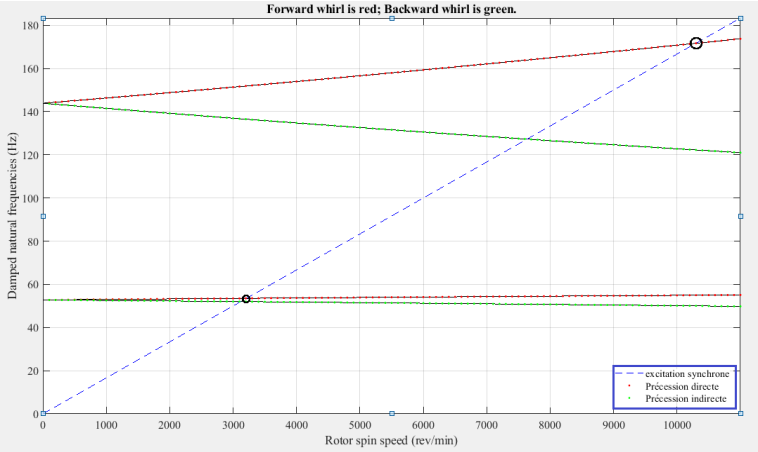

Figure2: Campbell diagram.

The amplitudes and direction of the whirlings at the level of nodes 2 (disk carrier) and 3 free are observed in following figure 3.

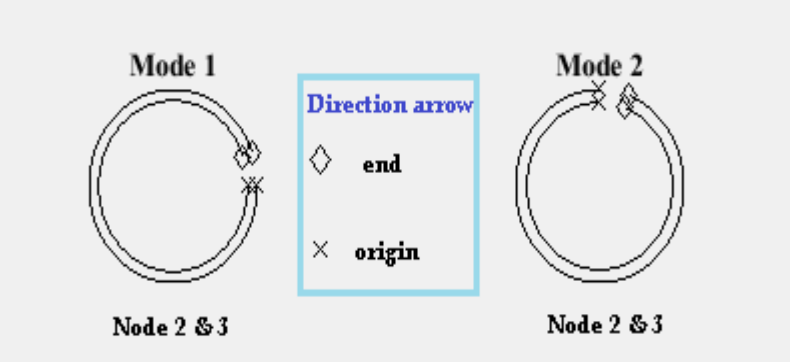

Figure 3:Amplitude and direction of whirlings at nodes 2 & 3.

The frequencies and modes corresponding to the two critical speeds cr_1 and cr_2 are observed in following figures. 4 and 5, in order to avoid them so as not to cause the system to resonate.

Vol. 7, No. 02; 2022

ISSN: 2456-3676

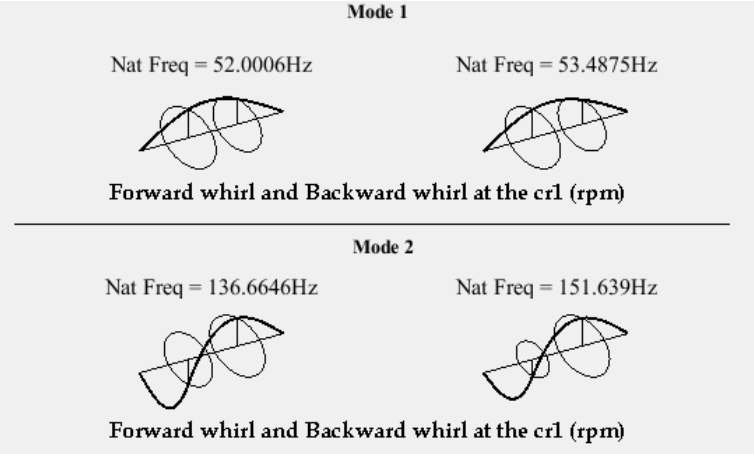

Figure4:The frequencies and modes corresponding to the first critical speed cr_1

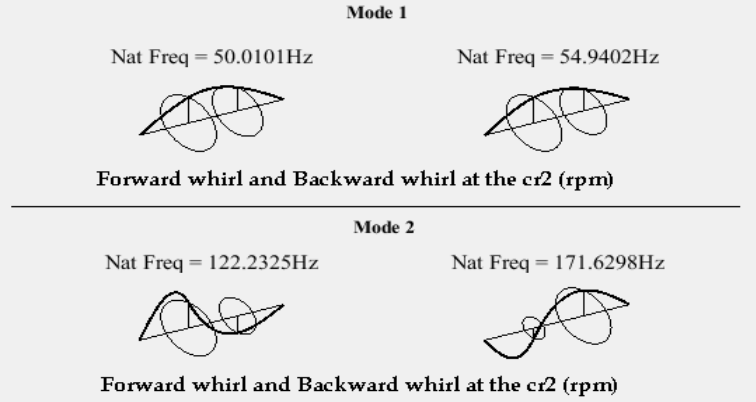

Figure5: The frequencies and modes corresponding to the second critical speed cr2

Discussion

Our efforts in this study focused on modeling the dynamic behavior of a flexible rotor, using the finite element method. The application of Lagrange's equations made it possible to determine the equations of motion for the finite element model. It gives a more complete discretization and description of the system to be studied thanks to a large number of degrees of freedom. It is used to predict the dynamic behavior of complex and industrial rotors. Finally, a simulation of the model made it possible to bring clarity to the critical speeds using the Campbell diagram, and the curves of frequencies and modes corresponding to these speeds which were considered as dark points.

Conclusion

In order to improve the performance and in particular the efficiency of industrial machines (brushless motor), the prediction of the dynamic behavior of the components of rotating machines must be carried out carefully.

Vol. 7, No. 02; 2022

ISSN: 2456-3676

All of the information obtained by the equations of motion and the various frequency and mode curves constitute factors that must be considered for correct operation of the motor; and improve the critical points finally to have a better performance.

References

BACHSCHMID N., PENNACCHI P., TANZI E. Cracked Rotors. Berlin : Springer, 2010.

GENTA G. Vibration of structures and machines. New York: Springer, 1995.

GENTA G. Dynamics of rotating systems. New York: Springer, 2005.

LALANNE M., FERRARIS G. Rotordynamics prediction in engineering. Chichester: Wiley, 1998.

RAO J.S. Rotordynamics. New York: Wiley, 1992.

DUCHEMIN, Matthieu. contribution à l'étude du comportement dynamique d'un rotor embarqué. Lyon : Ecole doctorale des sciences pour l'ingénieur de lyon, 2003.

YAMAMOTO T., ISHIDA Y. Linear and nonlinear rotor dynamics: A modern treatment with

applications. New York: Wiley, 2001.

GUILLAUME, Mogenier. Identification et prévision du comportement dynamique des rotors feuilletés en flexion. Lyon : INSA de Lyon, 2012. Thèse.

BOUKHALFA, Abdelkrim. Comportement vibratoire des arbres tournants en matériaux composites. Tlemcen : UNIVERSITE ABOU BEKR BELKAID, 2009. Thèse.

SINO, Rim. COMPORTEMENT DYNAMIQUE ET STABILITE DES ROTORS. Lyon: l'Institut National des Sciences Appliquées de Lyon, 2007. Thèse. N°d'ordre 2007-ISAL–0067.

Zaki, Dakel. Stabilité et dynamique non linéaire de rotors embarqués. Lyon : INSA de Lyon, 2014. Thèse de doctorat. NNT.

Medour, M. Dynamique de machines tournantes: 2ème Année Master,ConstructionMecanique. 2019.

M.I. Friswell, J.E.T. Penny, S.D. Garvey and A.W. Lees. Dynamics of Rotating Machines: Cambridge University Press, 2010.